ISSN 1070-3284, Russian Journal of Coordination Chemistry, 2018, Vol. 44, No. 7, pp. 460–465. © Pleiades Publishing, Ltd., 2018.

One Dinuclear Copper(II) Polymer Based on *N*-(Pyridine-3-Sulfonyl Amino)-Acetate: Synthesis, Structure, and Magnetic Analysis[1]

P. P. Yang[a], **S. X. Yang**[a, b], **X. J. Wei**[a, b, *], **M. Q. Chen**[a, b],
M. Z. Yang[a, b], **X. H. Yang**[a, b], **and X. H. Zhang**[c, *]
[a]*Guangxi Normal University, Guilin, 541004 P.R. China*
[b]*Huaihua Haitian High School, Huaihua, 418000 P.R. China*
[c]*Guangxi Key Laboratory of Comprehensive Utilization of Calcium Carbonate Resources,*
School of Materials and Environmental Engineering, Hezhou University, Hezhou, 542899 P.R. China
**e-mail: ppyanggxnu@163.com*

Received September 2, 2017

Abstract—The reaction of $CuCl_2 \cdot 2H_2O$ with *N*-(pyridine-3-sulfonyl amino)-acetate (H_2L) in ethanol, water and 4,4'-Bipy under solvothermal conditions leads to the formation of a dinuclear copper polymer $\{[Cu_2(L)_2(4,4'\text{-Bipy})(H_2O)_2] \cdot H_2O \cdot CH_3OH\}_n$ (**I**). The polymer was characterized by elemental analysis, IR spectroscopy, thermogravimetric analysis, and X-ray single-crystal diffraction (CIF file CCDC no. 1543747). The results showed that polymer belongs to the triclinic system, $P\bar{1}$ space group. TG curve shows that polymer **I** first removes water molecules, and then the ligand split for polymers **I**, and the remained residue is CuO. The magnetic measurement reveals the *N*-(pyridine-3-sulfonyl amino)-acetate as bridge ligand can mediate the antiferromagnetic coupling interaction between magnetic centers.

Keywords: polymer, *N*-(pyridine-3-sulfonyl amino)-acetate, structure, magnetic

DOI: 10.1134/S1070328418070023

INTRODUCTION

In recent years, design and synthesis of the paramagnetic transition polymetallic cluster since the discovery of "single-molecule magnets" (SMMs) are attractive to researchers [1–5], and the field of SMMs is developing very fast. How to design and synthesize SMMs is the key to magnetic materials. In the previous work [6–8], the scientist have been reported and studied antiferromagnetic coupling interaction between magnetic centers and found that *N*-[(3-pyridine)-sulfonyl]-aspartate can act as excellent building blocks with charge and multi-connecting ability in the construction of functional coordination polymers with porosity, photoluminescent or magnetic properties [9–11]. Generally, there are many factors that affect self-assembly of coordination assemblies: such as chemical structure of the ligands chosen, the coordination geometry preferred by the metals ions, the reaction temperature and the solvent system, the counter ions and the methods of crystallization [12–16]. Compared with the previously investigated *N*-[(3-pyridine)-sulfonyl]-aspartate ligands, herein, we choosing *N*-(pyridine-3-sulfonyl amino)-acetate (H_2L) and 4,4'-Bipy as reagent, obtained one dinuclear copper polymer $\{[Cu_2(L)_2(4,4'\text{-Bipy})(H_2O)_2] \cdot H_2O \cdot CH_3OH\}_n$ (**I**). This polymer was characterized by elemental analysis, IR spectroscopy, X-ray single-crystal diffraction, thermogravimetric and magnetic analysis.

EXPERIMENTAL

Physical measurements. All solvents and chemicals were commercial reagents and used without further purification. *N*-(Pyridine-3-sulfonyl amino)-acetate was synthesized according to references [9]. Elemental analyses (carbon, hydrogen, and nitrogen) were performed with a Perkin-Elmer 240 elemental analyzer. IR spectra were measured from KBr pellets on a Nicolet 5DX FT-IR spectrometer. The thermogravimetric (TG) analysis was determined by PerkinElmer Pyris Diamond TG-DTA. The crystal structure was determined by a Bruker APEX-II CCD. The magnetic measurements were carried out with a Quantum Design MPMS-XL7 and a PPMS-9 ACMS magnetometer.

Synthesis of I. A mixture of $CuCl_2 \cdot 2H_2O$ (0.0742 g, 0.2 mmol), H_2L (0.0872 g, 0.4 mmol), in 10 mL distilled water and 10 mL ethanol, the mixture was reaction for 10 min under 50°C then adjusted the

---

[1] The article is published in the original.

Table 1. Crystallographic data and structure refinement information for **I**

Parameter	Value
Formula weight	797.52
Temperature, K	293(2)
Crystal system	Triclinic
Space group	$P\bar{1}$
a, Å	7.6288(7)
b, Å	9.5197(7)
c, Å	10.9327(9)
α, deg	99.444(2)
β, deg	96.588(3)
γ, deg	93.515(2)
Volume, Å^3; Z	775.44(11); 1
ρ_{calc}, g cm^{-3}	1.789
μ, mm^{-1}	1.59
Limiting indices	$-9 \le h \le 9$, $-12 \le k \le 11$, $-14 \le l \le 14$
F(000)	430
θ Range for data collection, deg	3.1–25.0
Reflections collected/unique	7591/2370
R_{int}	0.041
Crystal size, mm	0.21 × 0.23 × 0.12
R ($F^2 > 2\sigma(F^2)$)	0.055
wR (F^2)	0.152
S	1.04
$(\Delta/\sigma)_{max}$	0.001
$\Delta\rho_{max}/\Delta\rho_{min}$, e Å^{-3})	1.66/–0.81

pH to 6 with triethylamine, continue to reaction for 3 h, added 0.048 g 4,4'-Bipy and 5 mL ethanol, continue heating for 4 h, then filtered, and obtained blue solution. The blue solution was natural evaporation at room temperature, the blue bulk crystal were obtained from the mother liquor after 15 days later. The yield was 91% (based on Cu).

For $C_{25}H_{30}N_6O_{12}S_2Cu_2$			
Anal. calcd., %	C, 37.62	H, 3.76	N, 10.53
Found, %	C, 37.61	H, 3.80	N, 10.55

X-ray crystallography. Blue bulk single crystals of polymer **I** having approximate dimensions of 0.21 × 0.23 × 0.12 mm was mounted on the top of a glass fiber. The diffraction data for polymer **I** were measured on a Bruker SMART diffractometer equipped with a graphite-monochromatized MoK_α radiation ($\lambda = 0.71073$ Å) at 293(2) K. A total of 7591 reflections were collected in the range of ($-9 \le h \le 9$, $-12 \le k \le 11$, $-14 \le l \le 14$), of which 2370 are unique ($R_{int} = 0.041$), and with $I > 2\sigma(I)$ were used in the refinement of the structure of polymer **I**. The anisotropic displacement parameters were applied to all non-hydrogen atoms in full-matrix least-squares refinements based on F^2 were performed SHELXL-2013. The structure was solved by direct methods using Olex2 program [17] and refined with Olex2 program [18]. Anisotropic thermal parameters were assigned to all non-hydrogen atoms. The hydrogen atoms were placed at calculated positions and refined as riding atoms with isotropic displacement parameters. Crystallographic crystal data and structure processing parameters for polymer **I** are summarized in Table 1. Selected bond lengths and bond angles for polymer **I** are listed in Table 2, hydrogen bonds for polymer **I** are listed in Table 3.

Supplementary material for **I** has been deposited with the Cambridge Crystallographic Data Centre (CCDC no. 1543747; deposit@ccdc.cam.ac.uk or http://www.ccdc.cam.ac.uk).

RESULTS AND DISCUSSION

The smallest independent unit of polymer **I** is shown in Fig. 1. The asymmetric unit consists of two Cu^{2+} ions, two deprotonated L^{2-} ligand, one 4,4'-Bipy, two coordinated water molecules, one free water and methanol molecule.

Table 2. Selected bond lengths (Å) and bond angles (deg) for **I***

Bond	d, Å	Bond	d, Å	Bond	d, Å
Cu(1)–N(3)	2.031(4)	Cu(1)–N(1)	1.976(5)	Cu(1)–N(2A)	2.001(4)
Cu(1)–O(5)	2.327(4)	Cu(1)–O(1)	1.962(3)		
Angle	ω, deg	Angle	ω, deg	Angle	ω, deg
N(1)Cu(1)N(3)	166.82(16)	N(2A)Cu(1)N(3)	91.90(17)	N(2A)Cu(1)N(1)	96.74(17)
O(5)Cu(1)N(3)	92.03(15)	O(5)Cu(1)N(1)	96.86 16)	O(5)Cu(1)N(2A)	96.37(15)
O(1)Cu(1)N(3)	86.45(15)	O(1)Cu(1)N(1)	82.91(15)	O(1)Cu(1)N(2A)	167.13(15)
O(1)Cu(1)O(5)	96.45(13)	C(5)N(2)Cu(1A)	122.6(3)	C(1)N(2)Cu(1A)	118.6(3)

* Symmetry code: (A) $-x + 2, -y + 1, -z + 2$.

Table 3. Geometric parameters of hydrogen bonds of polymer **I***

D–H···A	Distance, Å			Angle D–H···A, deg
	D–H	H···A	D···A	
O(5)–H(5a)···O(3*C*)	0.85	2.04(1)	2.886(5)	173(1)
O(6)–H(6)···O(4*D*)	0.82	2.2(2)	2.734(18)	123(3)
O(7)–H(7a)···O(2*E*)	0.85	2.10(1)	2.893(9)	155(1)

* Symmetry codes: (*C*) $-x + 1, -y + 1, -z + 2$; (*D*) $x, y, z - 1$; (*E*) $x, y - 1, z - 1$.

In polymer **I**, the Cu^{2+} ions is coordinated by three nitrogen atoms (N(1), N(2*A*) and N(3)) and two oxygen atoms (O(1) and O(5)). These three nitrogen atoms are derived from 4,4'-Bipy and the amino group and pyridine ring of L^{2-}, and two oxygen comes from water molecule and the carboxyl group of L^{2-}. It is worth noting that the oxygen on the carboxyl group takes a monodentate coordination style to coordinated with center Cu^{2+} ions and forms a chelated five-membered ring with the coordinated nitrogen atoms of 4,4'-Bipy and L^{2-}. The coordination pattern of the ligand is the structure of the reverse direction, the first and the end (N, O) are connected with different central Cu^{2+} ions (Fig. 1). The center Cu^{2+} ions in **I** are five-coordinated. For polymer **I**, the Cu–O distances fall in the range of 1.962(3) to 2.327(4) Å (the distances of Cu(1)–O(1) 1.962(3), Cu(1)–O(5) 2.327(4) Å). The Co–N distance fall in the range of 1.976(5) to 2.031(4) Å (Cu(1)–N(1) 1.976(5), Cu(1)–N(2*A*) 2.001(4), Cu(1)–N(3) 2.031(4) Å). These bond distances all fall in the normal ranges [19, 20]. The bond length and bond angle indicate that the central Cu^{2+} ion coordination environment is a slightly distorted tetrahedral geometry (Fig. 2).

In polymers **I**, the carboxyl groups in L^{2-} are coordinated in monodentric style, and the 4,4'-Bipy molecule is coordinated by μ_2-η^1:η^1 bridging style, so these two pyridine rings are almost in the same plane. And the coordination mode of the ligand is a *cis*-inverted structure, which is connected with the central ions to form a ring (Cu···Cu 7.3719(7) Å). In the ring, the plane 1 and 2 of pyridine ring of L^{2-} are parallel to each other, and the center distance of these two pyridine rings is 5.354(0) Å (Fig. 3) , and the vertical distance is 2.767(5) Å. Indicating that the polymer **I** had intramolecular π···π effect to make the molecules more stable. The adjacent ring was through the 4,4'-Bipy bridge to form a one-dimensional chain structure (Fig. 4). This structure is similar to the reported in the literature using 4,4-Bipy as bridged ligand [21].

Owing to the introduction of water molecules, polymers **I** had a large number of hydrogen bonds. It not only have intramolecular hydrogen bonds, but also have intermolecular hydrogen bonds. The free water molecule and methanol molecule are present in the molecule through intramolecular hydrogen bonds. These hydrogen bonds finally generating a three-

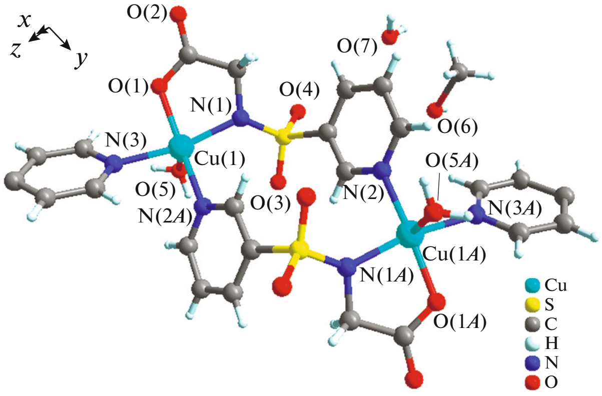

Fig. 1. The smallest independent unit of **I**.

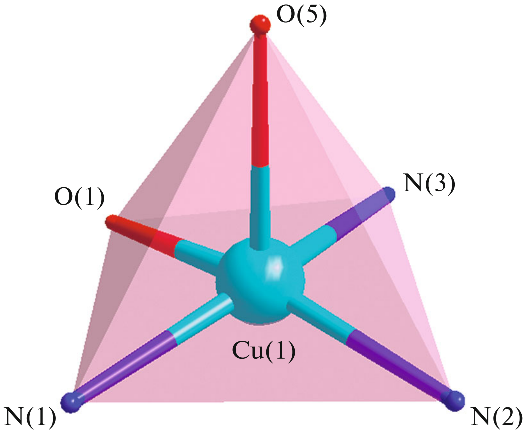

Fig. 2. The center Cu(II) deformed tetrahedral configuration of **I**.

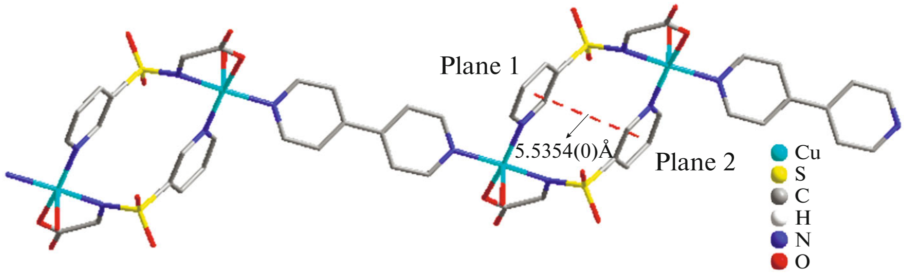

Fig. 3. The effect of intramolecular π···π.

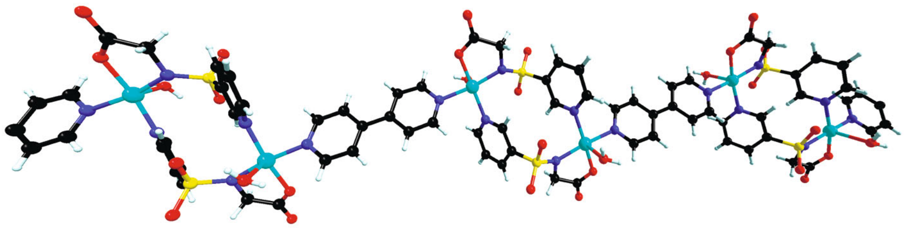

Fig. 4. The one-dimensional chain structure of **I**.

dimensional network structure along *x* axis by intermolecular hydrogen bonds (Fig. 5).

In order to check the purity of polymer **I**, powder X-ray diffraction of the as-synthesized sample was measured at room temperature. The peak positions of experimental patterns are in good agreement with the simulated ones (Fig. 6), which clearly indicates good purity of the polymer **I**.

The thermal stability of polymer **I** was tested in the range of 45–1000°C under a nitrogen atmosphere at a heating rate of 5°C $\min^{-1}$ for Pyris Daimond TG-DTG Analyzer. The TG curves of polymer **I** was shown in Fig. 7. The thermal gravimetric analysis curve show that the polymer **I** first loses of water molecules and methanol molecule (obsd. 9.82%, calcd. 10.78%) in the range of 45 to 173°C; further weight loss, responsible for all organic components in the range of 173 to 752°C; the last remaining amount of CuO (obsd. 20.52%, calcd. 19.93%).

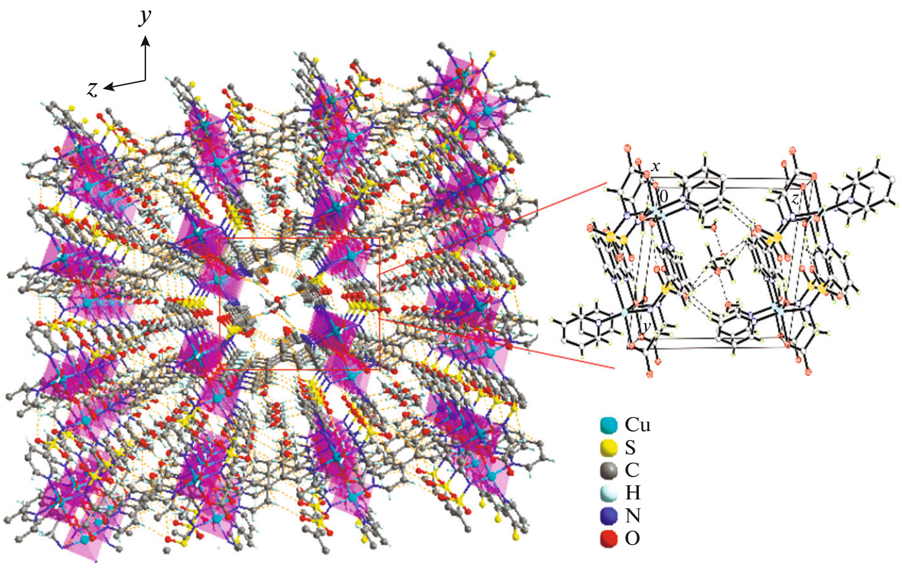

Fig. 5. The three-dimensional stacked structure was formed by hydrogen bonds.

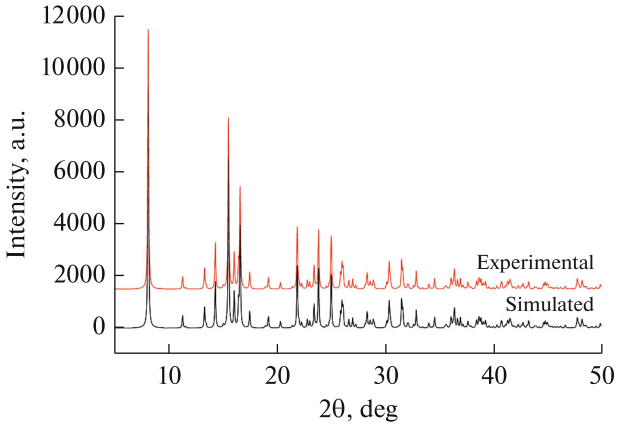

Fig. 6. The powder diffraction of polymer **I**.

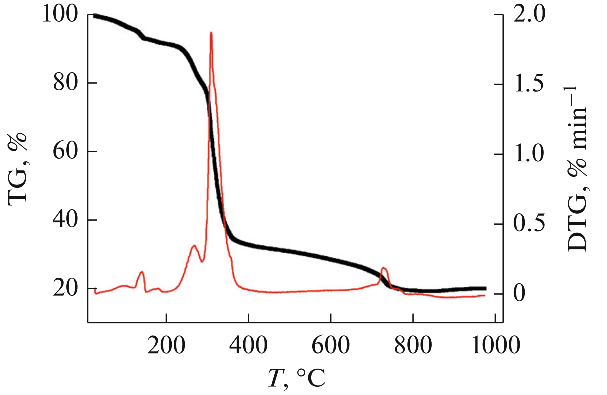

Fig. 7. The TGA of polymer **I**.

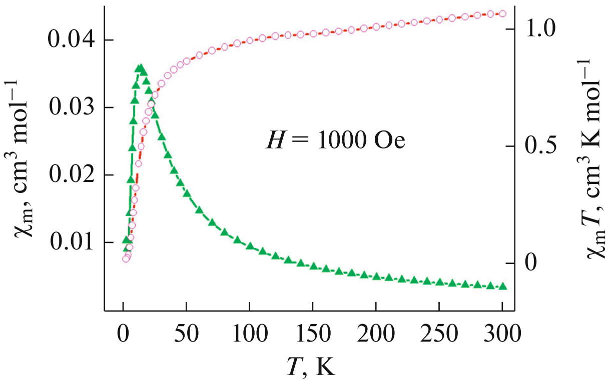

Fig. 8. χ_m, $\chi_m T$ vs. T of polymer **I**.

Polymer **I** is a Cu^{2+} (d^9) polymer having unpaired electrons, so its magnetic properties are studied. The magnetic susceptibilities (χ_m) of **I** were measured in the 2–300 K temperature range, and shown as χ_m and $\chi_m T$ versus T plots in Fig. 8. As seen in Fig. 8, the molar magnetic susceptibility χ_m of polymer **I** increases gradually as the temperature lowers, and more rapidly increases below 25 K, then reaches a maximum value of 0.01 cm^3 mol^{-1} at 2 K. It can be seen from the $\chi_m T$ curve that the $\chi_m T$ value is 1.06 cm^3 mol^{-1} K at 300 K, which is significantly lower than the theoretical value 1.88 cm^3 mol^{-1} K of the high-spin triplet Cu^{2+} (J = 4.92 cm^{-1}, g = 2.02), indicating a great spin-orbit coupling contribution. As the decrease of temperature, the $\chi_m T$ began to decrease slowly, and the decrease in the range of 300–25 K could be attributed to the single ion behavior of Cu^{2+}, but more rapidly reduction below 25 K, then reaches a minimum value of 0.02 cm^3 mol^{-1} K at 2 K. Combined with the decrease in the $\chi_m T$ value when cooling, this result indicates the presence of weak antiferromagnetic interactions in polymer **I** [22]. At 300 K, $\chi_m T$ = 1.06 cm^3 mol^{-1} K, the magnetic moment (μ_{eff}) of copper(II), which is determined by the equation $\mu_{eff} = 2.828(\chi_m T)^{1/2}$, reaches the peak value of 2.92 μ_B. This value is slightly higher than that expected for an isolated divalent high-spin Cu(II) system with μ_{eff} = 1.88 μ_B.

ACKNOWLEDGMENTS

The authors acknowledge the financial support from the National Natural Science Foundation of China (no. 51474077), Guangxi Scientific Research and Technology Development Program (GuikeAA16380042) and Guilin Scientific Research and Technology Development Program (no. 2016010502-2).

REFERENCES

1. Rinehart, J.D. and Long, J.R., *Chem. Sci.*, 2011, vol. 2, p. 2078.
2. Zhang, S.H., Zhang, Y.D., Zou, H.H., et al., *Inorg. Chim. Acta*, 2013, vol. 396, p. 119.
3. Zhang, S.H., Huang, Q.P., Zhang, H.Y., et al., *J. Coord. Chem.*, 2014, vol. 69, p. 3155.
4. Meihaus, K.R. and Long, J.R., *Dalton Trans.*, 2015, vol. 44, p. 2517.
5. Wang, J.H., Zhang, S.H., Wang, W., et al., *J. Clust. Sci.*, 2015, vol. 26, p. 1129.
6. Liao, B.L., Li, S.X., Guo, J.J., et al., *Russ. J. Coord. Chem.*, 2016, vol. 42, p. 285. doi 10.1134/S1070328416040035
7. Liao, B.L., Li, S.X., Yin, X.J., et al., *Chin. J. Inorg. Chem.*, 2016, vol. 32, p. 1255.
8. Jia, J.J., Zhang, L.K., Li, S.X., et al., *Chin. J. Struct. Chem.*, 2017, vol. 36, p. 266.
9. Shi, L.L. and Qin, F., *J. Jianghan Univ. (Nat. Sci. Ed.)*, 2007, vol. 35, p. 44.
10. Li, S.X., Liao, B.L., Yang, G.G., et al., *Synth. React. Inorg. Nano. Chem.*, 2015, vol. 45, p. 926.
11. Jia, J.J., Li, S.X., Yin, X.J., et al., *Russ. J. Inorg. Chem.*, 2017, vol. 62, p. 63. doi 10.1134/S0036023617010181

12. Fang, R.Q. and Zhang, X.M., *Inorg. Chem.*, 2006, vol. 45, p. 4801.
13. Rarig, R., and Zubieta, J.R.J., *Dalton Trans.*, 2001, vol. 23, p. 3446.
14. Eddaoudi, M., *Science*, 2002, vol. 295, p. 469.
15. Stock, N. and Bein, T., *Angew. Chem. Int. Ed.*, 2004, vol. 43, p. 749.
16. Pan, L., Frydel, T., Sander, M.B., et al., *Inorg. Chem.*, 2001, vol. 40, p. 1271.
17. Dolomanov, O.V., Bourhis, L.J., Gildea, R.J., et al., *J. Appl. Cryst.*, 2009, vol. 42, p. 339.
18. Bourhis, L.J., Dolomanov, O.V., Gildea, R.J., et al., *Acta Crystallogr., Sect. A: Found. Adv.*, 2015, vol. 71, p. 59.
19. Liao, B.L., Li, S.X., Luo, P., and Jiang, Y.M., *Inorg. Nano-Met. Chem.*, 2017, vol. 47, no. 2, p. 213.
20. Li, S.X., Luo, P., and Jiang, Y.M., *Russ. J. Coord. Chem.*, 2017, vol. 43, no. 4, p. 238. doi 10.1134/S1070328417040042
21. Ma, L.F., Wang, L.Y., Huo, X.K., et al., *Cryst. Growth Des.*, 2008, vol. 8, no. 2, p. 620.
22. Jeter, D.Y., Hodgson, D.J., and Hatfield, W.E., *Inorg. Chem.*, 1972, vol. 11, p. 185.